Advances in Science and Technology Research Journal

Advances in Science and Technology Research Journal, 2025, 19(9), 353–368
https://doi.org/10.12913/22998624/207695
ISSN 2299-8624, License CC-BY 4.0

Received: 2025.06.09
Accepted: 2025.07.15
Published: 2025.08.01

Modification of PVC plastisol with silver nanoparticles to obtain protective materials with antibacterial properties

Joanna Kowalik[1*], Magdalena Tworek[1], Anna Ligocka[2], Magdalena Osial[3]

[1] Faculty of Chemical Engineering and Technology, Bydgoszcz University of Science and Technology, ul. Seminaryjna 3, 85-326 Bydgoszcz, Poland
[2] Faculty of Agriculture and Biotechnology, Bydgoszcz University of Science and Technology, Al. Prof. S. Kaliskiego 7, 85-796 Bydgoszcz, Poland
[3] Faculty of Chemistry, University of Warsaw, ul. Pasteura 1, 02-093 Warsaw, Poland
* Corresponding author's e-mail: joanna.kowalik@pbs.edu.pl

ABSTRACT

In this work, we developed and characterized the membranes based on polyvinyl chloride plastisol modified with silver nanoparticles deposited on silica. The aim of the study was to obtain a functional PVC plastisol composite for use as linings and protective coatings, with improved mechanical, thermal, and antimicrobial properties. The plastisol was prepared by mixing PVC resin with a plasticizer (bis(2-ethylhexyl) adipate). Silver nanoparticles were produced by two methods: chemical reduction using sodium citrate and gum arabic, and these particles were deposited on Aerosil®200 silica. These composites were introduced into plastisol at different concentrations and then processed into films by gelation and hydraulic pressing. The formation of silver nanoparticles was confirmed by UV-Vis spectrophotometry, and the morphology of the composites was examined by scanning electron microscopy. Further characterization of the materials included infrared spectroscopy, thermomechanical analysis, mechanical property testing, and thermogravimetric analysis. Mechanical properties such as Young's modulus, tensile strength, and elongation at break were determined by static tensile tests. Shore hardness tests were also performed to evaluate the stiffness of the composites. The antimicrobial activity of the membranes was evaluated according to ASTM method E2149-01 using reference strains of *S. aureus* and *E. coli.* Studies have shown that silver nanoparticles effectively inhibited the growth of *E. coli*, especially at higher concentrations of AgNPs, while they had no effect on *S. aureus*. AgNPs modified membranes obtained from the reduction of $AgNO_3$ with sodium citrate and deposited on silica showed higher microbiological activity than those with AgNPs reduced with gum arabic. An optimal filler content in the range of 1 to 1.5% provides the most favorable combination of mechanical, thermal, and antibacterial properties.

Keywords: plastisol, silver nanoparticles, fumed silica.

INTRODUCTION

PVC plastisol pastes used to be an underestimated part of polyvinyl chloride, but have now become a highly desirable material. PVC plastisol is a type of plastic combining suspended emulsion PVC particles in a liquid plasticizer. It exhibits a number of interesting physical and chemical properties, such as flexibility, durability, and chemical resistance. Plastisol pastes can be modified by adding stabilizers, pigments, fillers, and other additives that give the finished coating the right properties. They affect the way the PVC plastisol flows, which is important when selecting the coating application method. The most commonly used methods are coating, spraying, injection molding, and rotational molding [1, 2]. After heating, the viscosity increases due to the absorption of the plasticizer by the PVC particles, which creates a flexible material that is resistant to stretching, resistant to changing weather conditions and at the same time has good decorative values [3–5]. PVC plastisol coatings are also characterized by excellent chemical resistance and are dielectrics. In the past, they were mainly used for the production of paste for caps and screw caps. Currently, they are a very good material for casting or coating various surfaces such as non-woven fabrics, metals, wood [6]. Plastisol coatings also create functional external layers that are used in everyday life or in specific, difficult conditions in the automotive industry as protective coatings for vehicle chassis [2]. The areas of application are very diverse and depend primarily on the composition of the PVC plastisol. Application in the textile, footwear or medicine industries [7–9].

The latest technological solutions taking into account environmental protection and safety have led to many innovative applications of PVC plastisol products. The latest compositions of PVC coatings are primarily aimed at minimizing the use of health-hazardous plasticizers such as phthalates. Due to serious negative health effects, their use has been restricted in the European Union and several other countries [10, 11]. Many works have described bioplasticizers, which include plasticizers based on lactic acid, vegetable oil and waste vegetable oil, polyester plasticizers, adipates, citrates, etc. [12–15]. Inorganic and organic fillers of natural origin are used as additives to PVC plastisol. Fillers primarily affect changes in mechanical properties, improve resistance to external factors, improve optical properties, change rheological properties and reduce the costs of the finished product. The most commonly used fillers are calcium carbonate, kaolin, titanium dioxide and silica [16]. Many authors have investigated the effect of organic fillers [17–20] and mineral fillers [21–23] on changes in mechanical properties and rheology of plastisol pastes. The subject of numerous studies is the modification of polymer materials with filler particles, which provide many functional properties, such as optical properties [24], bactericidal and antifungal effects [25, 26]. Studies of polymer composites with the addition of metal nanoparticles are particularly popular in science [27]. These include, among others, materials containing silver nanoparticles, which, as is commonly known, belong to antibacterial and antifungal agents. Thanks to numerous studies, many materials with specific properties for various applications have been developed. For example, Vance et al. [28] developed a list of consumer products containing nanomaterials, including AgNPs, Liu et al. [29], Hu et al. [30] described the effectiveness of dressing materials and hydrogels with silver nanoparticles in wound treatment, Przemieniecki et al. [31] demonstrated the effect of AgNPs on the soil microbiome, and numerous publications on their use in agriculture as plant protection products [32, 33, 34], Assis et al. [35] obtained a PVC-SiO_2-Ag composite that also eliminates SARS-CoV-2 for use in everyday devices such as smartphones, glasses, etc. However, silver nanoparticles are unstable in physiological conditions, they aggregate and lose their antimicrobial activity. Therefore, they can be dispersed on metal and nonmetal oxides to form composites. In such forms, they have a wide range of applications, including energy conversion and environmental applications [36] and in coating materials with antibacterial properties [37–42].

The research undertaken in this work aimed to obtain a PVC plastisol composite for use as linings and protective coatings. An additional objective was to demonstrate the favorable physicomechanical properties, and above all, the antibacterial effectiveness of the developed material. A more environmentally and health-friendly plasticizer in the form of bis (2-ethylhexyl) adipate was used for the research. Silver nanoparticles were obtained by chemical reduction and applied to Aerosil® 200 fumed silica. The membranes obtained from the modified plastisol were subjected to mechanical and thermal tests. The antibacterial properties of the produced materials were also assessed in relation to Gram-positive and Gram-negative bacteria.

MATERIALS AND METHODS

Materials

To prepare the plastisol, an emulsion poly(vinyl chloride) called Vinnolit E-2059 was used, with a K number of 59, reduced viscosity of 86.0 $cm^3 \cdot g^{-1}$ and density of 0.520 $g \cdot cm^{-3}$, manufactured by Vinnolit GmbH Co. KG, Carl-Zeiss-Ring 25, Ismaning, Germany. Bis (2-ethylhexyl) adipate with the trade name Ergoplast ADO, manufactured by Boryszew S.A., Sochaczew Branch, Poland, was used as a plasticizer. Plasticizer properties: molecular weight of 370 $g \cdot mol^{-1}$, density of 0.924 $g \cdot cm^{-3}$, viscosity of 13 mPas. To obtain silver nanoparticles deposited on silica, hydrophilic fumed silica Aerosil® 200 from Evonik Operations GmbH, Germany, with a surface area of 200 $m^2 \cdot g^{-1}$, silver nitrate (V) p.a. from Avantor Performance Materials Poland S.A., Gliwice, sodium citrate p.a. from Avantor Performance Materials Poland S.A., Gliwice, and spray-dried gum arabic from Pharma Cosmetic K.M. Adamowicz sp. z o.o., Kraków, Poland were used.

Preparation of plastisol poly(vinyl chloride)

The plastisol was prepared by preliminary mixing in a mortar 800 g of powdered PVC polymer with 880 g of ADO plasticizer. The whole was mixed for 2 hours daily. After mixing, the plastisol was degassed each time at rest in a HZV vacuum dryer at a pressure of 6.5 hPa and a temperature of 20 °C. The cycles were repeated for 21 days. After this time, the plastisol was rubbed on a triple-roller EXAKT 50I from EXAKT Advanced Technologies GmbH, Germany, with a roller diameter of 50 mm. The speed/roller ratio was 1.8, and the gap settings were 5 and 3. The plasticizer used solvated and dissolved the poly(vinyl chloride) grains, which is confirmed by the homogeneous mass formed, which did not contain air bubbles.

Preparation of silver nanoparticles

Silver nanoparticles were obtained by chemical reduction using sodium citrate and gum arabic as reducing agents. The reagents were weighed on a RADWAG AS220.R2 laboratory scale with an accuracy of 0.1 mg. The formation of AgNPs was confirmed by spectrophotometric methods. The obtained Ag nanoparticles were deposited on Aerosil®200 silica. The description of the methods is presented below:

- Method 1 – the $AgNO_3$ solution with a concentration of 1mM was heated to a temperature of 95 ± 5 °C. A previously prepared 3 mM sodium citrate solution was poured into the silver nitrate solution with continuous stirring. The pH of the reaction mixture was maintained between 8 and 9. The solution quickly changed color to yellow and then to brown. The whole was heated and stirred for 2 hours. The solution was cooled to room temperature, and then 11 g of silica was added as a carrier for AgNPs. The suspension was stirred for 15 minutes. The whole was dried in an oven at 90 ± 2 °C for 12 hours.
- Method 2 – a 3 wt% aqueous solution of gum arabic was prepared and heated to 90 ± 3 °C. A weighted amount of $AgNO_3$ corresponding to a solution concentration of 0.006 mM was added to the solution. The pH of the solution ranged from 7.5 to 8.5. The mixture was stirred continuously for 2 hours at 500 rpm. Then the solution was set aside for another hour. The color change from a colorless mixture to tea color indicated the presence of silver nanoparticles. 11 g of silica was added to the solution as a carrier for AgNPs. The suspension was stirred for 15 minutes, then dried in a dryer at 90 ± 2 °C for 12 hours.

Preparation of PVC plastisol membranes with silver nanoparticles on silica

Up to 50 g of PVC plastisol was introduced 1; 1.5; 2% by weight of silica with AgNPs obtained by two methods. All samples were rubbed three times on a three-roller EXAKT 50I under the same conditions as the PVC plastisol. The obtained compositions were gelled in an oven at 140 °C for 60 minutes. The films prepared in this way were placed in a hydraulic press in a pressing mold. The films were pressed under a pressure of about 50 bar at a temperature of 140 °C to a thickness of 2 mm. The obtained films were circular in shape with a diameter of 180 mm and a thickness of 2 mm, from which samples were taken for further tests.

Methods

UV-VIS spectrophotometry

Confirmation of AgNPs formation was performed by spectrophotometric absorption measurements using a SHIMADZU UV-1280 UV-VIS spectrophotometer. The analysis was performed over the wavelength range of 300–750 nm. The presence of silver nanoparticles was confirmed by the absorption maximum observed between 380 and 450 nm. Prior to the UV-Vis measurements, the AgNPs solutions were diluted.

Scanning electron microscope

The morphology of the plastisol-based composites and the inorganic filler were analyzed using scanning electron microscopy (SEM) – Zeiss Merlin Zeiss GmbH, Oberkochen, Germany, where prior to the morphology studies the samples were coated with the thin gold layer to maintain uniform conductivity of the material while analysis.

FTIR spectroscopy

Infrared (FTIR) spectroscopic studies of silver nanoparticle (AgNPs) samples were performed using a Bruker Alpha-P spectrometer equipped with a diamond attenuated total reflectance (ATR) accessory. The OPUS 6.5 software was used for spectral acquisition. The measurements were carried out in the wavenumber range of 350–4000 cm^{-1}, with a spectral resolution of 4.0 cm^{-1}. The tests were carried out on modified PVC films. No additional sample preparation was required. Infrared radiation was transmitted through the crystal and partially absorbed at the sample–crystal interface. The attenuated beam was then directed to the detector for analysis.

Shore hardness of coatings

The hardness of PVC plastisol films with Aerosil® 200 silica modified with silver nanoparticles was measured using a Shore A device from Zwick Roell, Ulm, Germany according to the PN EN 868-2003 standard [43]. The material hardness was measured after 15 seconds at 5 measurement points. The hardness result is the arithmetic mean of all measurements.

Thermomechanical tests

Thermomechanical tests were carried out using a Höppler consistometer from VEB MLW Prüfgerate-Werk Medingen/Sitz, Germany. Measurements were taken in the temperature range from 20 to 140 °C at a load of 494 g. The deformation degree was read at a temperature increase rate of 2.0 °C min^{-1}. The test results were presented as graphs of the dependence of deformation under a given load on temperature. The experiments were repeated on two samples.

Mechanical properties

The mechanical properties were tested in static tension using an Instron 5966 testing machine at a tension speed of 30 $mm \cdot m^{-1}$. Strips of 110 × 2 mm and 100 mm in length were cut from the films. The tests were conducted on three samples. The tests were used to determine Young's modulus, tensile strength of the films and elongation at break.

Thermogravimetric analysis

Thermogravimetric analysis of the membranes was performed using a Netzsch TG 209 F3 Tarsus device. The tests were performed in a nitrogen atmosphere in the temperature range of 30 to 900 °C with a rate of change of 10 $°C \cdot min^{-1}$. The initial decomposition temperatures, the temperature corresponding to the first and second decomposition maximum, the temperature of the maximum decomposition rate and the final decomposition temperatures were determined. The temperature values were determined from the intersection of the extrapolated baseline and the tangent of the inflection of the TGA and DTG lines. Netzsch Proteus – Thermal Analysis (version 4.8.5), dedicated to the TGA device, was used to determine these values. The mass losses of the tested samples during the first and second stages of decomposition were determined.

Microbiological tests

The antimicrobial activity of the membranes was assessed based on the American Society for Testing and Materials (ASTM) E2149-01 method [44]. Two reference strains of microorganisms from the American Type Cell Culture (ATCC) collection were used - *Staphylococcus aureus* ATCC 6538P (Gram-positive bacteria) and *Escherichia coli* ATCC 25922 (Gram-negative bacteria). The membranes from samples 1 to 7 were cut into 1.5 cm squares and each side was disinfected using UV-C radiation (25 minutes each). The microorganisms were cultured on TSA medium (Tryptic Soy Agar, Merck 22091) at 37 °C for 24 hours. After this time, standardized bacterial suspensions of 0.5 McFarland density were prepared in sterile physiological saline solution and further diluted to 107 CFU/ml to obtain a working suspension. Suspensions of each bacterium together with a small amount of TSB medium were introduced into eight sterile flasks (10 ml each), and then carriers were placed in them: carrier with sample 1, carriers with samples 2–4, carriers with samples 5–7. One of the samples was a suspension without carrier as a control for the growth of the inoculum itself. All samples were placed in a shaking incubator (INC 125 FS digital (SP20) Incubator shaker) at 37 °C, 80 rpm, and the number of microorganisms was determined at time 0 and after 1, 3 and 24 h. For this purpose, 1 ml of suspension was taken from each flask, which was diluted in 0.85% NaCl in the range of 10-1-10-7 and plated on selective media. For *E. coli* bacteria, it was ENDO medium (Merck, 104044), and for *S. aureus*, Chapman medium (Merck 105404). Incubation was carried out at 37 °C for 24–48 h, after which the number of microorganisms in the initial samples was determined and expressed in log10. The reduction in the number of microorganisms (CFU) was also calculated by subtracting the logarithmized number of CFU of the test samples from the log10 CFU in the control samples.

RESULTS

UV-VIS analysis of the obtained silver nanoparticles

UV-VIS studies showed absorption maxima at 400 nm and 420 nm, which confirms the presence of silver nanoparticles in the obtained solutions after chemical reduction. The plasma band is quite wide, which may be caused by the uneven size distribution of AgNPs particles. Different peak intensities reflect changes in the concentrations of silver nanoparticles (Figure 1).

Morfology of of the plastisol-based composites and the inorganic filler

PVC plastisol and AgNPs-modified silica were used to obtain films with different filler contents. The properties of the finished coating materials largely depend on the composition and method of obtaining the plastisol paste. 0.5; 1; 1.5; 3; 5; 7 and 10% of silica with AgNPs were introduced into the plastisol. Based on preliminary studies, it was found that films containing 5% or more of the filler showed a lack of continuity and delamination. For this reason, plastisol compositions with lower filler contents were selected for further studies. Figure 2 shows SEM images of silver nanoparticles on silica obtained by method 1 (Figure A) and method 2 (Figure B) and cross-sections of samples of pure PVC plastisol and silica-modified plastisol films with deposited silver nanoparticles. The morphology of the plastisol-based composites and the inorganic filler were analyzed using SEM – Zeiss Merlin Zeiss GmbH, Oberkochen, Germany, where prior to the morphology studies the samples were coated with the thin gold layer to maintain uniform conductivity of the material while analysis. Figure 2 A-B shows the bare inorganic filler obtained with two different techniques. As can be seen, both silica suspensions modified with the AgNPs reveal the granular structure-based aggregates. The differences in brightness result from the uneven overlapping of individual grains. The following images were captured for plastisol-based composite filled with the abovementioned structures in different wt.%, in particular 1, 1.5, and 2% wt%. Composite samples were broken in half after cooling in liquid nitrogen and the cross-section was analyzed. Figure 2 C shows the homogeneous structure of unmodified PVC plastisol, while the following figures present the composite filled with the silica-AgNPs particles. As can be seen in Figure 2 D-F demonstrate the composite with the filler obtained with method 1 for 1, 1.5, and 2% wt%, respectively, where the aggregates of the silica-AgNPs can be distinguished. The higher the content of silica results in the aggregates in the composite cross-section. As a result of the differences in the hydrophilicity of the composite components. The effect can be caused by the varied hydrophilicity of the composite ingredients. At the same time, the observed differences in the filler distribution can be caused by the degassing of the PVC plastisol composite during sample preparation. The observed differences in filler distribution may be due to the sample preparation process. In future studies, the process

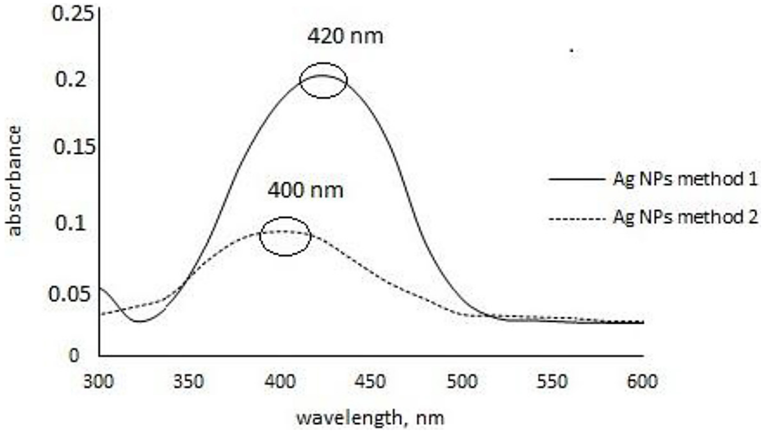

Figure 1. UV-VIS spectrum of AgNPs obtained by 1 and 2 method

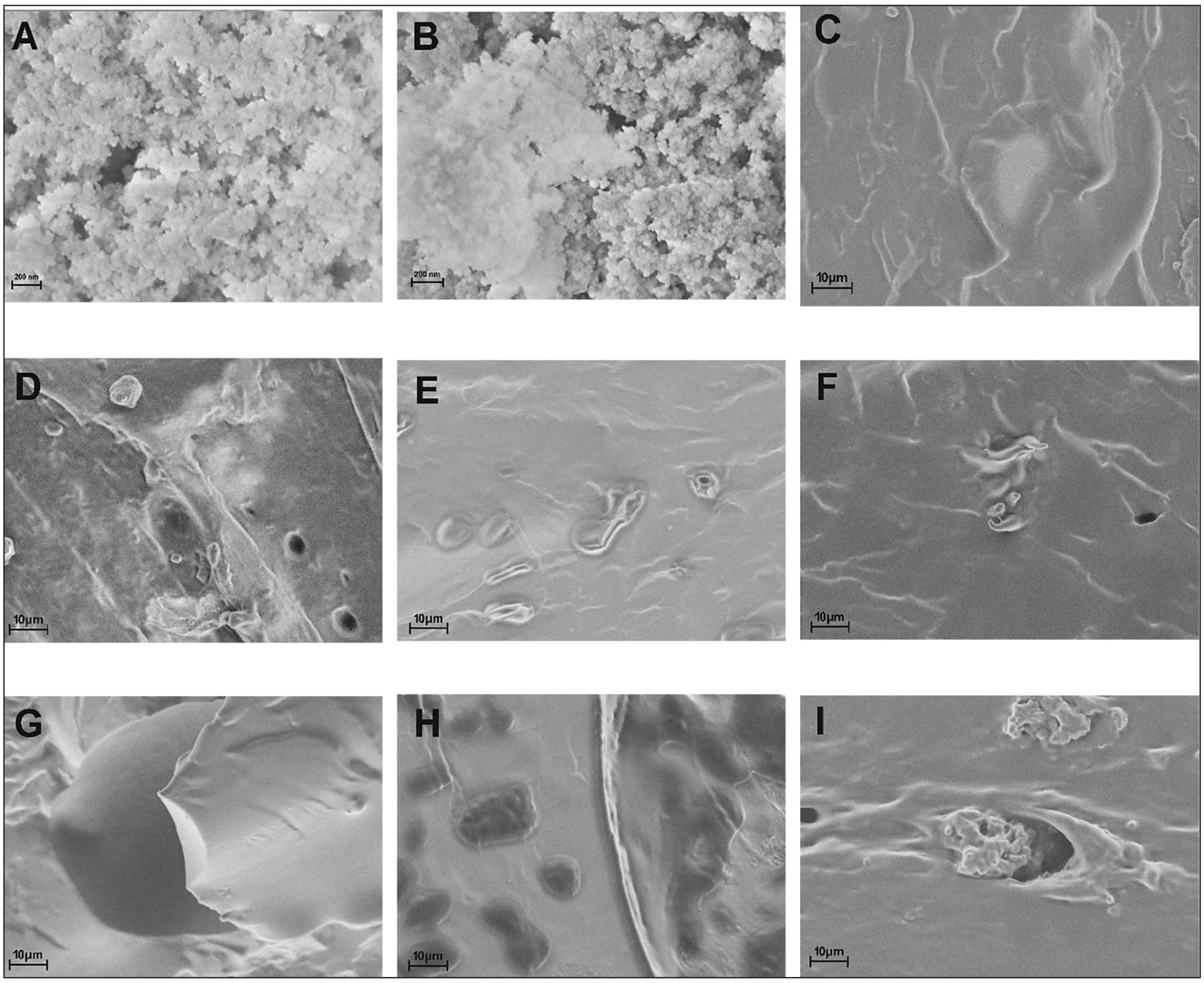

Figure 2. SEM images of (A) Aerosil® 200 silica suspension modified with AgNPs obtained with procedure 1, (B) procedure 2, (C) PVC plastisol, and PVC plastisol modified with silica suspension modified with AgNPs obtained with procedure 1 with (D) 1% wt%, (E) 1.5% wt., (F) 2% wt., and silica suspension modified with AgNPs obtained with procedure 2 with (G) 1% wt., (H) 1.5% wt., and I) 2% wt.%

of silica distribution in the polymer matrix should be improved. Images presented in Figure 2 G-I show films with the highest homogeneity for the 1% wt% of the filler, while the higher wt% results in the non-uniform distribution of the filler in the composite. SEM images provided valuable information on the homogeneity of the films to be included in the following studies, especially when it comes to mechanical studies.

Hardness test results of PVC plastisol compositions

In order to assess the quality and durability of the coatings, hardness tests of the obtained films were carried out. Table 1 presents the compositions of the tested PVC plastisol compositions and the results of hardness measurements. Hardness tests show that as the content of silica with AgNPs increases, the hardness of the films decreases. The films containing Ag nanoparticles obtained by method 2 have lower hardness than those obtained by method 1.

Thermomechanical deformation of modified PVC plastisol

Thermomechanical tests consisted in determining the deformation of a modified PVC plastisol sample under the action of a constant load, which was recorded as a function of temperature in the form of a thermomechanical curve. The tests were performed on a Höppler consistometer, recording the deformation of a 6 mm thick sample under the influence of the load. The study was started at an initial temperature of 20 °C, and subsequent strain measurements were taken at 2 °C intervals. The initial section of the

Table 1. Composition of the tested PVC plastisol compositions modified with Aerosil® 200 silica with silver nanoparticles and the results of the film hardness test

Sample number	Plastizol/type of silver ion reducer	Aerosil® 200 silica percentage of AgNPs, %	Shore hardness, °Sh
1	Plastisol PVC	0	35.0
2	Plastisol PVC/SC	1.0	32.0
3	Plastisol PVC/SC	1.5	31.5
4	Plastisol PVC/SC	2.0	29.5
5	Plastisol PVC/GA	1.0	29.5
6	Plastisol PVC/GA	1.5	26.5
7	Plastisol PVC/GA	2.0	19.0

thermomechanical curve corresponded to the elastic state region, where the thermal energy of the polymer macromolecules was too low to cause deformation under load. The onset of deformation of the pure PVC plastisol was observed at 60 °C, while in the case of plastisols modified with silica with the addition of silver nanoparticles (AgNPs), this temperature decreased to 50 °C. It was observed that the higher the silica content in the composition, the lower the deformation onset temperature. These are the designated temperatures of the so-called heat resistance, which determine the temperatures of the actual usability of the polymer. This is the temperature to which the polymer can be heated without the risk of its significant softening. When examining the relationship between deformation and temperature in samples 2 to 4, no significant changes in deformation were

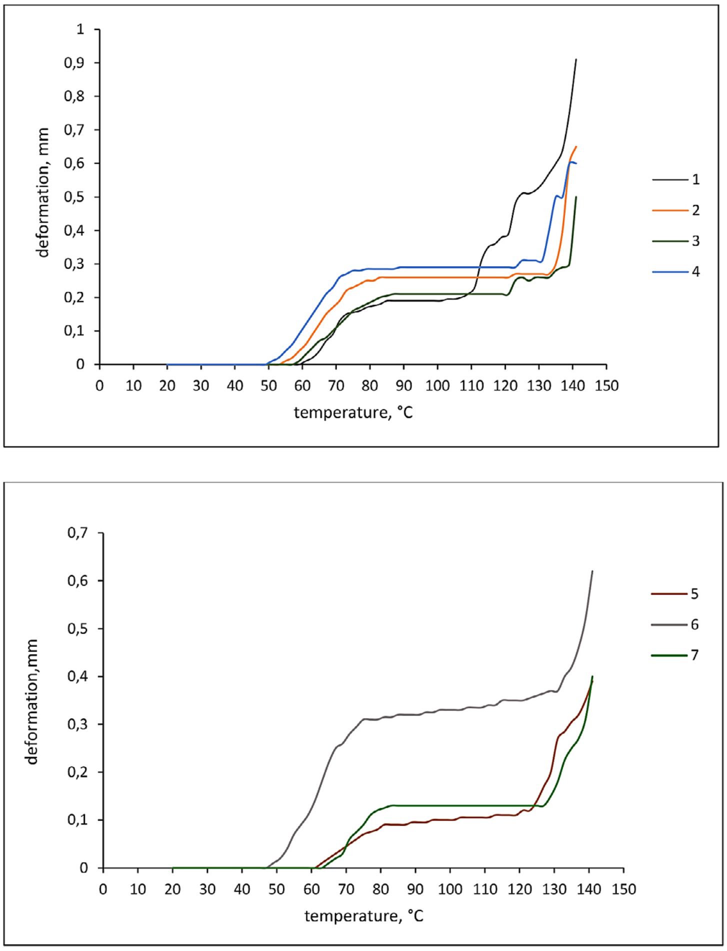

Figure 3. Temperature dependence of strain for PVC plastisol films and PVC plastisol modified with silica suspension modified with AgNPs

observed depending on the content of silica with AgNPs obtained by the first method. In the case of PVC plastisol composites modified with silica with AgNPs obtained by method 2, a lower deformation value of 0.1 mm was observed for samples 5 and 7. A further increase in temperature caused an increase in deformation and a transition to the liquid state. The flow temperature of the pure plastisol was 110 °C, and the modified plastisol was higher and ranged from 123–133 °C for samples 5–7 and from 130–139 °C for samples 2–4 (Figure 3). Table 2 presents the softening and flow temperatures of the tested PVC plastisol compositions.

Mechanical properties of PVC plastisol with nanoparticles

During use, PVC plastisol composites are subjected to various mechanical factors. Therefore, tensile strength tests were performed at break, its elongation and a parameter characterizing the stiffness of the material Young's modulus were determined. Figure 4 shows the values of Young's modulus, tensile strength at break and relative elongation of PVC plastisol modified with silica with silver nanoparticles.

The data presented in the figure show that the PVC plastisol membrane was characterized by the highest value of relative elongation. Similar elongation values were found in compositions containing 1 wt.% of silica with AgNPs (sample 2 and 5). The elongation at break decreased with the increase in the amount of filler. The membranes with 1 and 1.5 wt.% filler had higher tensile strength than the membrane with unmodified plastisol. This strength decreased with the increase in the amount of filler in the membrane. The Young's modulus of the plastisol depends on many factors, such as temperature, chemical composition and degree of plasticization. This is an important utility parameter. The Young's modulus of the modified membranes was 2.7 to 3.8 MPa, and of the PVC plastisol itself 1.5 MPa. The Young's modulus decreased with the increase in the amount of filler. The exception is sample 6 containing 1.5% of silica with silver nanoparticles obtained by method 2. The studies showed that the best strength properties were possessed by films 2, 3 and 5 containing 1 and 1.5% by weight of filler. Higher filler content caused deterioration of mechanical properties, which was caused by weaker adhesion at the interface between the filler and the polymer. In these films, discontinuities in the polymer structure were also observed in

Table 2. Determined softening and flow temperatures of PVC plastisol films and modified composites

Sample numer	Softening temperature, °C	Flow temperature, °C
1	80	110
2	75	135
3	86	139
4	72	130
5	80	123
6	71	133
7	79	128

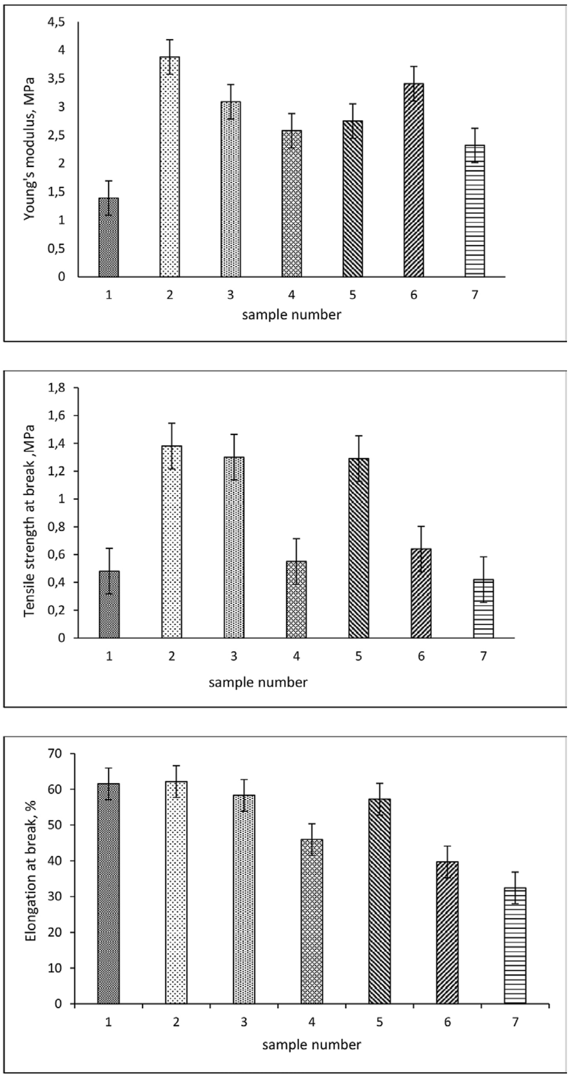

Figure 4. Young's module, tensile strength at break and relative elongation of PVC plastisol films and films modified with silica-supported silver nanoparticles as a function of nanoparticle content

the form of empty spaces, which is confirmed by SEM images. The even distribution of silica in the polymer matrix also had an impact on mechanical properties. In the plastisol containing 2% or more of silica with silver nanoparticles, the mechanical properties of the plastisol deteriorated.

Studies of polymer-plasticizer interactions using infrared spectroscopy

Good polymer-plasticizer miscibility is essential for effective plasticization of poly(vinyl chloride) and obtaining coating materials with desired thermal and mechanical properties. Using infrared spectroscopy, the compatibility of PVC-plasticizer resulting from physical interactions between the components was investigated (Figure 5).

In the spectrum, characteristic for poly(vinyl chloride) bands of 2800–2900 cm^{-1} stretching vibrations of the asymmetric (-CH$_2$-) group, deformation vibrations –CH in the range of 1250–1430 cm^{-1} and a band of 600–700 cm^{-1} stretching vibrations of the C- Cl bond were observed, which indicates an unchanged structure of the main PVC chain. The spectrum shows characteristic bands of the ester plasticizer in the form of a band of 1735 cm^{-1} for carbonyl groups of esters, a band of 1120–1170 –COC- groups in esters and a band of –CH groups from 2870–2950 cm^{-1} of alkyl chains. Spectra in the range of 1900–2400 cm^{-1} of samples with different filler content differ slightly in the magnitude of transmittance. Clear changes are visible in the range of 1900–2800 cm^{-1}, where there are bands corresponding to hydroxyl groups, multiple bonds, etc. formed as a result of oxidation reactions. In the range of 1000–1100 cm^{-1}, there are indeed intense signals, but they can also be attributed to the ester vibrations C–O–C present in the matrix, related to the presence of the plasticizer. In the range of ~800 cm^{-1}, only weakly outlined signals are visible, which may correspond to C–Cl vibrations from PVC, and not unequivocally to Si–O groups. The lack of clear, intense bands indicates that the content of silica in the sample was probably very low or the signals from silicon could have been masked by intense vibrations of organic groups in the polymer matrix (PVC and plasticizer).

Thermal stability

To investigate the synergistic effects of the additives on the thermal stability and degradation behavior of the resulting composite films, thermal analysis was performed. Figure 6 presents the DTG curves of the thermal decomposition of neat PVC and PVC containing silver nanoparticles supported on silica.

From the thermogravimetric curves, the initial temperature, the temperature of maximum degradation rate, and the final degradation temperature were determined, along with the corresponding mass loss of the samples. Table 3 summarizes the individual degradation stages of the PVC plastisol membranes and the composites modified with silica-supported AgNPs.

In the temperature range from 20 to 1000 °C, two stages of sample mass change occur. Each stage is assigned a temperature corresponding to the initial decomposition, a temperature at which the maximum rate of decomposition occurs, and a temperature marking the end of decomposition.

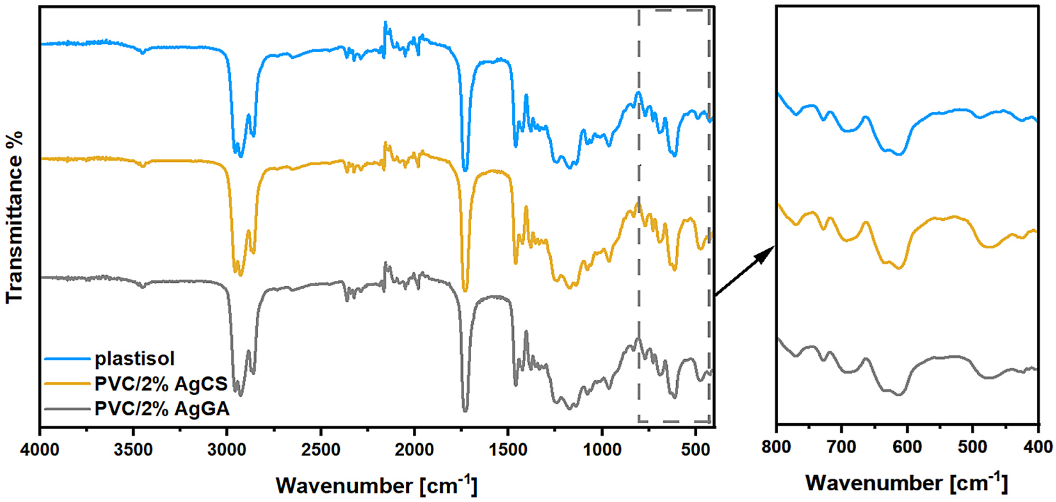

Figure 5. The spectra of PVC plastisol and compositions modified with silica with AgNPs

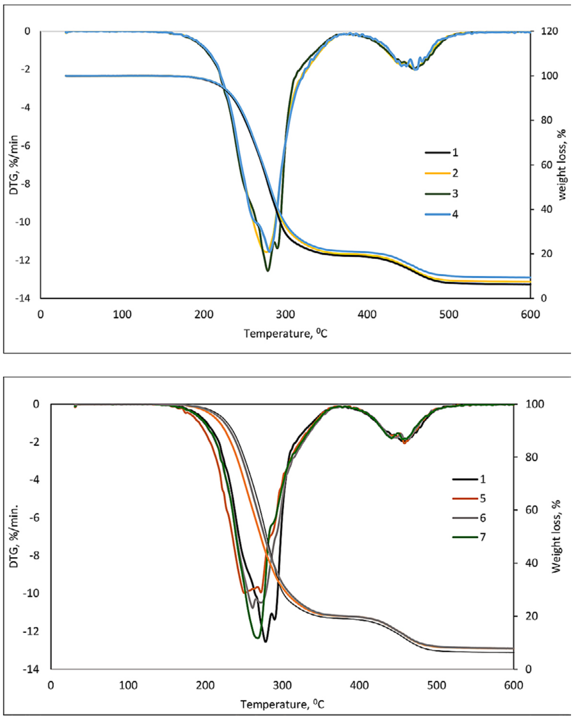

Figure 6. Thermogravimetric curves of mass changes of plastisol films and their composites with silver nanoparticles modified silica

The percentage change in mass is also recorded. All PVC plastisol samples exhibit similar initial decomposition temperatures. In the range from 150 °C to 400 °C, the main mass loss (80 wt%) takes place. This is due to the dehydrochlorination of PVC, resulting in the formation of polyene sequences along the PVC polymer backbone. The second stage, from 400 °C to 520 °C, involves a mass loss of about 10 wt%, associated with the decomposition of polyene sequences and the generation of carbon residues. The presence of Ag-NPs reduced by sodium citrate (Ag/SC) does not alter the degradation mechanism of the plastisol. The addition of silver nanoparticles reduced by gum arabic (Ag/GA) slightly enhances the thermal resistance of the plastisol. Degradation occurs within a similar temperature range, but the process is more distributed and less rapid. This may be due to the stabilizing effect of silver nanoparticles, which influence the polymer degradation mechanism, for example, by limiting the mobility of free radicals or interacting with the polymer matrix.

Microbiological tests

The results of microbiological tests clearly indicate that only *E. coli* (Gram-negative) was sensitive to the antimicrobial effect of nanosilver contained in both types of membranes (Figure 6, 7). Antibacterial efficacy was correlated with the percentage of silica with AgNPs in the plastisol, which was most clearly visible in the case of the PVC composite obtained by method 1 after 24 hours of contact with *E. coli* cells. The effect of antibacterial action appeared after 3 hours, but it was definitely weaker than at the end of the experiment. As can be seen from Table 4, the strongest antimicrobial effect after 24 hours was

Table 3. Transformation temperature values for the first and second stage of decomposition of the tested materials, where Tp — initial decomposition temperature, Tm — inflection temperature, the highest decomposition rate, and Tk — final temperature

Sample number	Decomposition stage	Initial decomposition temperature, T_i, °C	Temperature of maximum decomposition rate, T_{max}, °C	Final decomposition temperature, T_f, °C	Weight change in wt%, (-) weight loss
1	1	157	277	396	-81.16
	2	397	455	509	-11.97
2	1	160	276	390	-80.18
	2	391	457	500	-11.71
3	1	157	277	374	-80.73
	2	374	455	513	-12.45
4	1	161	280	366	-78.6
	2	367	459	510	-11.38
5	1	155	250	368	-79.7
	2	369	447	513	-11.94
6	1	156	261	365	-79.52
	2	366	458	514	-12.03
7	1	159	267	372	-79.18
	2	373	455	521	-11.89

demonstrated by the plastisol with 2% silica with AgNPs, causing a reduction in the number of bacteria by almost 4 log compared to the control, and thus reducing the population of *E. coli* by 99.9%. Carriers with AgNPs at concentrations of 1% and 1.5% inhibited bacterial growth slightly less effectively; however, their antimicrobial activity remained very high, resulting in a 99.9% reduction in CFU in both cases.

The effect of the PVC plastisol modified with silica with AgNPs obtained by the second method turned out to be much weaker (Figure 8). Only the film with the highest content of silica with silver nanoparticles (sample no. 7) caused a decrease in the number of *E. coli* by 96.8% after 24 h of contact. Lower concentrations of AgNPs did not reduce the number of bacteria (Table 5).

Gram-positive bacteria – *S. aureus*, proved to be resistant to nanosilver in both types of membranes, regardless of its concentration (Figure 9, 10). A slight decrease in the bacterial population occurred only in the first hour of contact of cells with both types of membranes, with a stronger biocidal effect exerted by nanosilver obtained by method 2 in samples 6 and 7 at concentrations of 1.5 and 2% (population reduction by 24.09 and 89.7%, respectively) (Table 5).

DISCUSSION

The results of the studies showed that during the gelation of the PVC plastisol and modified composites, membranes with a network consisting of physically connected polymer chains and a homogeneous structure were obtained. The plasticizer used showed good solvation capacity, penetrated into the PVC grains causing their swelling and plasticization. This behavior is consistent with typical gelation processes described for plastisols based on PVC [45]. Studies on the hardness of the PVC plastisol composite membranes with

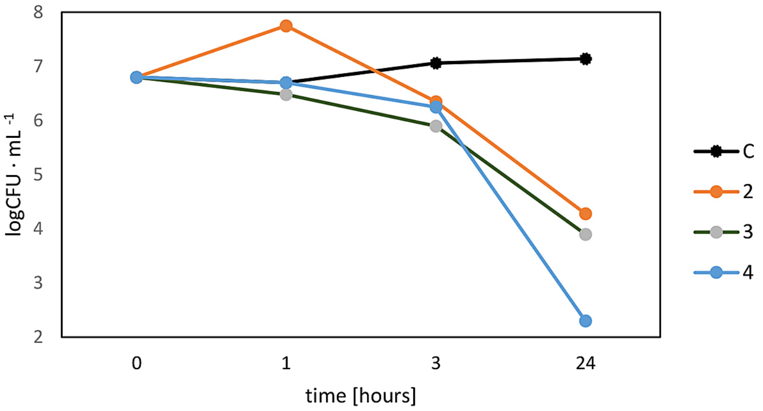

Figure 7. Number of *E. coli* cells in membrane medium with different silica content with silver nanoparticles obtained by method 1 and in control sample (C)

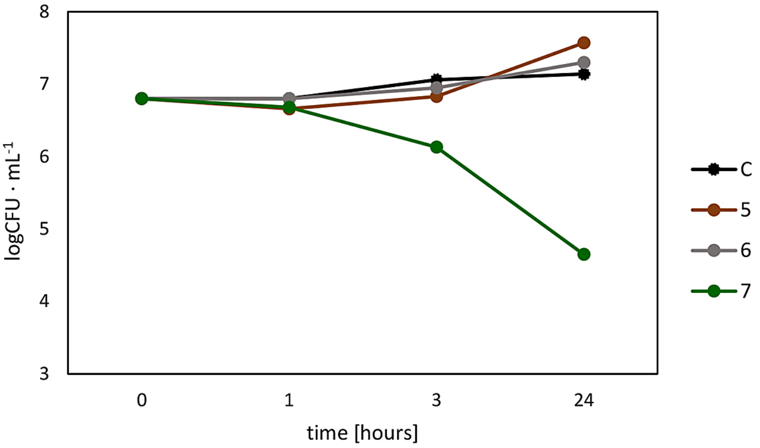

Figure 8. Number *of E. coli* cells in the membrane environment with different content of silica with silver nanoparticles obtained by method 2 and in the control sample (C)

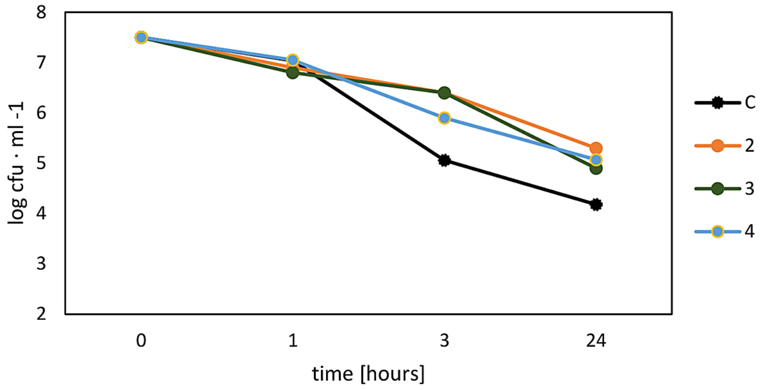

Figure 9. Number of *S. aureus* cells in the membrane environment with different contents of silica with silver nanoparticles obtained by method 1 and in the control sample (C)

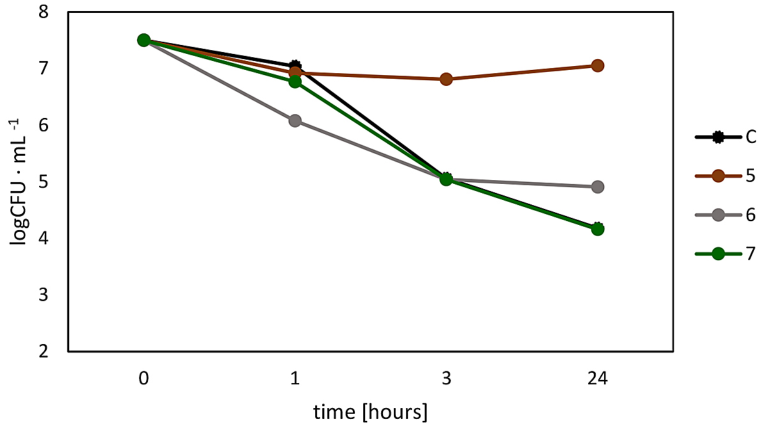

Figure 10. Number of *S. aureus* cells in the membrane environment with different contents of silica with silver nanoparticles obtained by method 2 and in the control sample (C)

Table 4. Effect of different concentrations and contact time of membranes on the reduction of bacterial populations

Bacteria	Sample number	Fumed silica percentage of AgNPs, % method 1 [wt%]	Contact time [hours]	Log reduction	% reduction
E. coli	2	1	1	0	0
			3	0.7	80.9
			24	2.9	99.9
	3	1.5	1	0	0
			3	0.6	73.9
			24	3.3	99.9
	4	2	1	0	0
			3	0.8	84.5
			24	3.8	99.9
S. aureus	2	1	1	0.1	27.3
			3	0	0
			24	0	0
	3	1.5	1	0.3	44.1
			3	0	0
			24	0	0
	4	2	1	0	0
			3	0	0
			24	0	0

Table 5. Effect of different concentrations and contact time of membranes on the reduction of bacterial populations

Bacteria	Sample number	Fumed silica percentage of AgNPs, % method 2 [wt%]	Contact time [hours]	Log reduction	% reduction
E. coli	5	1	1	0.1	6.1
			3	0.2	41.7
			24	0	0
	6	1.5	1	0	0
			3	0.1	22.6
			24	0	0
	7	2	1	0.02	4.1
			3	0.9	88.7
			24	1.5	96.8
S. aureus	5	1	1	0.1	24.1
			3	0	0
			24	0	0
	6	1.5	61	1.0	89.7
			3	0	0
			24	0	0
	7	2	1	0.3	47.3
			3	0.01	3.5
			24	0.02	3.3

the addition of silica with AgNPs showed that the hardness of the membranes decreased with the increase in the filler content. Similar effects were observed by Olgun et al. [46], who reported that increasing the content of AgNPs and silica in PCL-based films resulted in softening of the composite structure, despite improved antimicrobial functionality.

The results of SEM studies confirmed the homogeneous structure of the unmodified PVC plastisol membrane. In contrast, irregularly distributed clusters of silica particles with AgNPs were observed in the modified membranes. The more filler in the membrane, the more free spaces in the cross-section of the sample. Their presence affects the deterioration of the mechanical properties of the material, which has been previously reported in other polymer nanocomposites, where agglomeration of nanoparticles induced structural defects [47]. Therefore, the next research step will be to develop an appropriate method for dispersing the filler in the plastisol paste. Improved dispersion methods, including surface modification of fillers or use of compatibilizers, have been shown to enhance homogeneity and mechanical stability in similar systems.

The results of thermomechanical tests of membrane samples showed that the strain-temperature curve was influenced by the content of silica with AgNPs. An increase in the amount of filler in the membranes caused an increase in deformation and a slight decrease in the softening temperature of the composite and an increase in the flow temperature from about 15 to 30 °C. This indicates limited thermal stabilization and slight reinforcement, which is in agreement with previous studies on nanocomposites containing silver. Strength tests showed that the membranes containing 1% silica with AgNPs had a similar tensile strength at break as the plastisol membrane without filler. With an increase in the amount of filler, the strength gradually decreased. The relative elongation of the modified PVC plastisol was higher than that of the plastisol without filler. With an increase in the amount of filler, the elongation value decreased. An exception was the membrane with the addition of silica with AgNPs obtained by method 2 in the amount of 1.5%, which may be attributed to more stable particle dispersion or improved interaction between filler and matrix. The Young's modulus of the modified PVC plastisol membranes was higher than that of the PVC plastisol paste. Moreover, FTIR spectroscopic studies did not reveal any significant changes in the chemical structure of PVC or plasticizer, suggesting that the modification of the composite does not affect the basic chemical structure of the material. This agrees with findings from Long et al. [48] and Milczarek et al. [49] who observed that silver nanoparticles supported on silica do not chemically alter the matrix polymer but influence its morphology and performance. Thermogravimetric analysis showed that the presence of AgNPs in PVC-plastisol composites did not significantly affect the degradation mechanism of the material. However, silver nanoparticles obtained by method 2 (Ag/GA) slightly improved the thermal stability by changing the mass distribution during decomposition.

In the antimicrobial activity tests, PVC-plastisol composites with AgNPs showed high efficacy against *E. coli*, especially in the case of samples with 2% silica AgNPs content. The antimicrobial effect was much stronger in samples obtained by method 1, which may indicate better activity or availability of AgNPs against this bacterium. Similar trends were reported by Olgun et al. [46], where AgNPs combined with silica showed superior activity against Gram-negative bacteria. In the case of *S. aureus*, silver nanoparticles showed practically no bactericidal activity, suggesting that their action is specific to certain bacterial strains. This is also in line with findings from Long et al. [48], who noted that AgNPs supported on silica spheres had a much stronger effect on *E. coli* compared to Gram-positive bacteria.

CONCLUSIONS

The conducted studies have shown that the modification of PVC plastisol by adding silver nanoparticles deposited on silica significantly affects the physical, mechanical, thermal and antimicrobial properties of the obtained composites. The optimal filler content was about 1–1.5%, at which the best compromise between mechanical strength, thermal stability and biological effectiveness of the material was obtained.

Silver nanoparticles obtained by the reduction method using sodium citrate (Ag/SC) showed higher antimicrobial activity against *E. coli* compared to nanoparticles obtained using gum arabic (Ag/GA). At the same time, it was observed that increasing the amount of filler leads to deterioration of mechanical properties due to the presence of voids and agglomerates in the membrane structure. FTIR spectroscopy and thermogravimetric analysis confirmed that the modification process does not significantly affect the chemical structure of the PVC matrix or the plasticizer used, which indicates the physical nature of the modification. The obtained results confirm the validity of using silver nanoparticles in PVC composites as a component that gives the material antimicrobial properties, while maintaining favorable functional properties.

REFERENCES

1. Nugent P. Rotational Molding; Applied Plastics Engineering Handbook; Processing, Materials, and Applications Plastics Design Library, 2017, 321–343.
2. Savczenko B., Sova N., Beloshenko V., Debeluy B., Slieptsov A., Vozniak I. New approach for extrusion additive manufacturing of soft and elastic articles from liquid-PVC-based consumable materials, Polymers, 2022, 14(21), 4683, https://doi.org/10.3390/polym14214683
3. Pivsa-Art. S., Thanabat S., Phasuk G., Bumrungsuk T. Improvement of thermal stability of PVC plastisol dip mlding products, Annual Technical Conference – ANTEC, Conference Proceedings, 2014, 2197–2200.
4. Tworek, M., Skowronski, Ł., Makarewicz, E., Kowalik, J. Properties of UV-irradiated poly (vinyl chloride) membranes containing cadmium pigments, Scientific Reports, 2021, 11, 18165, https://doi.org/10.1038/s41598-021-96713-w
5. Keibal, N.A., Kablov, V.F., Stepanova, A.G., Ikryannikova, V.V. Development of a fire-resistant polyvinylchloride coating for the production of fire curtains. Journal of Applied Polymer Science. Serie D 2022, 15, 552–556, https://doi.org/10.1002/app.34647
6. Jabbari M., Akesson D., Taherzadeh M. Novel lightweight and highly thermally insulative silica aerogel-doped poly(vinyl chloride)- coated fabric composite, Journal of Reinforced Plastics and Composites, 2015, 34,19, https://doi.org/10.1177/0731684415578306
7. Vogt, W.C., Jia, C., Wear, K.A., Garra, B., Pfefer, T.J. Development and validation of a biologically realistic tissue-mimicking material for photoacoustics and other bimodal optical-acoustic modalities, Proceedings Volume 10056, Design and Quality for Biomedical Technologies X; 100560C, 2017, https://doi.org/10.1117/12.2254596
8. Jaime R.A.O., Basto R.L.Q., Lamien B., Eibner S., Fudym O. Fabrication methods of phantoms simulating optical and thermal properties, Procedia Engineering, 2013, 59, 30–36, https://doi.org/10.1016/j.proeng.2013.05.090
9. Muh W.S., Ina A., Indri H., Yayat I.S. Silica from geothermal waste as reinforcing filler in artificial leather, Key Engineering Materials, 2020, 849,

78–83, https://doi.org/10.4028/www.scientific.net/KEM.849.78

10. Wirnitzer, U., Rickenbacher, U., Katerkamp, A., Schachtrupp, A. Systemic toxicity of di-2-ethylhexyl terephthalate (DEHT) in rodents following four weeks of intravenous exposure. Toxicology Letters 2011, 205, 8–14, https://doi.org/10.1016/j.toxlet.2011.04.020
11. EU Commission Regulation (EU) 2018/2005, No 1907/2006. Available online: https://eur-lex.europa.eu/eli/reg/2018/2005/oj/eng, (accessed on 15 Januar 2025)
12. Filipiak B. Plasticizers in polymers: trends, health and ecology, 2016, Przemysł Chemiczny 1(11),237–241, https://doi.org/10.15199/62.2016.11.46
13. Zheming Z., Pingping J., Dekai L., Shan F., Pingbo Z., Yantao W., Junhong F., Agus A., Haryono A. Research progress of novel bio-based plasticizers and their applications in poly(vinyl chloride), Journal of Materials Science 2021, 56(17),1–28, https://doi.org/10.1007/s10853-021-05934-x
14. Stolp L.J., Grass M., Kodali D.R. Castor epoxy fatty acid alkyl ester estolides as bioplasticizers for poly(Vinyl Chloride), Journal of the American Oil Chemists' Society, 2021, 98, 297–304, https://doi.org/10.1002/aocs.12462
15. Perito E.D., Guerra N.B., J. da Silva Crespo. Chemical, thermal and mechanical evaluation of poly(vinyl chloride) plastisol with different plasticizers, Journal of Elastomers and Plastics, 2022, 58, 8, https://doi.org/10.1177/00952443221135001
16. Jaoua-Bahloul H., Varieras D., Beyou E. Solar spectra properties of PVC plastisol – based films filled with various fillers, Journal of Ninyl & additive Technology, 2018, https://doi.org/10.1002/vnl.21685
17. Siekierka P., Makarewicz E., Wilczewski S., Lewandowski K., Skórczewska K., Mirowski J., Osial M. Composite of poly (Vinyl Chloride) plastisol and wood flour as a potential coating material, Coatings, 2023, 13, 1892, https://doi.org/10.3390/coatings13111892
18. Torres–Giner, S., Montanes, N., Fennolar, O., Garcia-Sanoguera, D., Balart, R. Development and optimization of renewable vinyl plastisol/wood flour composites exposed to ultraviolet radiation, Materials & Design, 2016, 108, 648–658, https://doi.org/10.1016/j.matdes.2016.07.037
19. Georgopoulos, S.T., Tarantili, P.A., Avgerinos, E., Andreopoulos, A.G., Koukios, E.G. Thermoplastic polymers reinforced with fibrous agricultural residues. Polymer Degradation and Stability, 2005, 90, 303–312, https://doi.org/10.1016/j.polymdegradstab.2005.02.020
20. Crespo, J.E., Sanchez, L., Parres, F., López, J. Mechanical and morphological characterization of pvc plastisol composites with almond husk fillers, Polymer Composites, 2007, 28, 71–77, https://doi.org/10.1002/pc.20256
21. Abdesselam Y., Agassant J.F., Castellani R., Valette R., Demay Y., Gourdin D., Peres R. Reology of plastisol formulations for coating applications, Polymer Engineering and Science, 2016, 982–988, https://doi.org/10.1002/pen.24475
22. Maleki H., Durães L., Portugal A. An overview on silica aerogels synthesis and different mechanical reinforcing strategies, Journal of Non – Crystalline Solids, 2014, 385, 55–74, https://doi.org/10.1016/j.jnoncrysol.2013.10.017
23. Jaoua-Bahloul H., Zinet M., Beyou E., Blanc G., Varieras D. Numerical simulation of the solar spectral properties of filled polyvinyl chloride plastisols, Journal of Thermophysics and Heat Transfer, 2020, 34, 4, https://doi.org/10.2514/1.T5952
24. Shah, L.A., Ambreen, J., Bibi, I., Sayed, M., Siddiq, M. Silver nanoparticles fabricated hybrid microgels for optical and catalytic study. Journal of The Chemical Society of Pakistan, 2016, 38, 850–858.
25. Fu S., Sun Z., Huang P., Li Y., Hu N. Some basic aspects of polimer nanocomposites: A critical review, Nano Materials Science, 2019, 2–30, https://doi.org/10.1016/j.nanoms.2019.02.006
26. Kim D. Y., Patel S., Rasool K., Lone N., Bhatia S. K., eth C. S., Ghodake G. S. Bioinspired silver nanoparticle-based nanocomposites for effective control of plant pathogen: A review, Science of The Total Environment,, 2024, 908, 168318, https://doi.org/10.1016/j.scitotenv.2023.168318
27. Singh G., Sharma P.K., Malviya R. Biomedical applications and patents on metallic nanoparticles, Nanoscience & Nanotechnology-Asia, 2021, 153–162, https://doi.org/10.2174/2210681210999200430005827
28. Vance M.E., Kuiken T, Vejerano EP, McGinnis SP, Hochella MF, Hull DR. Nanotechnology in the real world: Redeveloping the nanomaterial consumer products inventory, Beilstein Journal of Nanotechnology, 2015, 6:1769–1780, https://doi.org/10.3762/bjnano.6.181
29. Liu T., Xie F., Geng L., He R., Sun M., Ni T., Xing C., Peng Y., Chen K., Fang Y. Micro-electro nanofibrous dressings based on PVDF-AgNPs as wound healing materials to promote healing in active areas, International Journal of Nanomedicine, 2025, 20, 771–789, https://doi.org/10.2147/IJN.S506489
30. Hu Q., Du Y., Bai Y., et al. Sprayable zwitterionic antibacterial hydrogel with high mechanical resilience and robust adhesion for joint wound treatment, macromolecular Rapid Communications, 2024,45(8):2300683, https://doi.org/10.1002/marc.202300683
31. Przemieniecki S. W., Ruraż K., Kosewska O., Oćwieja M., Gorczyca A. The impact of various

forms of silver nanoparticles on the rhizosphere of wheat (*Triticum aestivum* L.) – Shifts in microbiome structure and predicted microbial metabolic functions, Science of The Total Environment, 2024, 914, 169824, https://doi.org/10.1016/j.scitotenv.2023.169824

32. Bapat M. S., Singh H., et al. Evaluating green silver nanoparticles as prospective biopesticides: An environmental standpoint, Chemosphere, 2022, 286, 131761, https://doi.org/10.1016/j.chemosphere.2021.131761
33. Elbeshehy E., Elazzazy A., Aggelis G. Silver nanoparticles synthesis mediated by new isolates of Bacillus spp., nanoparticle characterization and their activity against Bean Yellow Mosaic Virus and human pathogens, Frontiers in microbiology, 2015, 6, 453, https://doi.org/10.3389/fmicb.2015.00453
34. Hazarika A., Yadav M., Yadav D., Yadav H. An overview of the role of nanoparticles in sustainable agriculture, Biocatalysis and Agricultural Biotechnology, 2022, 43, 102399, https://doi.org/10.1016/j.bcab.2022.102399
35. Assis M., Simoes L. G. et al. PVC-SiO_2- Ag composite as a powerful biocide and anti-SARS-CoV-2 material, Journal of Polymer Research, 2021, 28:361, https://doi.org/10.1007/s10965-021-02729-1
36. Patnaik S., Sahoo D. P., Parida K. An overview on Ag modified g-C3N4 based nanostructured materials for Energy and environmental applications, Renewable and Sustainable Energy Reviews, 2018, 82(1), 1297–1312, https://doi.org/10.1016/j.rser.2017.09.026
37. Zhou Y., Wang L., et al. Enhanced high thermal conductivity and low permittivity of polyimide based composites by core-shell Ag@SiO_2 nanoparticle fillers, Applied Physics Letters, 2012, 101,012903, https://doi.org/10.1063/1.4733324
38. Taheri S., Vasilev K., Majewski P. Silver nanoparticles: synthesis, antimicrobial coatings, and applications, Recent Patents on Materials Science, 2015, 8, 166–175, https://doi.org/10.2174/1874464808666150331222126
39. Vasilev K. Nanoengineered antibacterial coatingsand materials: A Perspective, Coatings, 2019, 9, 654, https://doi.org/10.3390/coatings9100654
40. Seyfi J., Panahi-Sarmad M., et al. Antibacterial superhydrophobic polyvinyl chloride surfaces via the improved phase separation process using silver phosphate nanoparticles, Colloids and Surfaces B: Biointerfaces, 2019, 183, 110438, https://doi.org/10.1016/j.colsurfb.2019.110438
41. Vasilev O., Hayles A., et al. Nanoscale antibacterial coating incorporating silver nanoparticles derived by plasma techniques- A state – of- the-art. Perspective, Materials Today Chemistry, 2024, 41, 102341, https://doi.org/10.1016/j.mtchem.2024.102341
42. Olgun U., Tunc K., Hos A. Preparation and antibacterial properties of nano biocomposite Poly(ε-caprolactone)-SiO2 films with nanosilver, Journal of Polymer Research, 2019, 26(2), https://doi.org/10.1007/s10965-018-1686-0
43. ISO 868:2003 Plastics and ebonite — Determination of indentation hardness by means of a durometer (Shore hardness)
44. ASTM E2149-01 Standard Test Method for Determining the Antimicrobial Activity of Antimicrobial Agents Under Dynamic Contact Conditions
45. Utracki, L.A., Polymer Blends Handbook. Springer, 2002.
46. Olgun U., Tunc, K., Özaslan V., Preparation of antimicrobial polycaprolactone-silica composite films with nanosilver rods and triclosan using roll-milling method, Polymers for Advanced Technologies, 2011, 22, 2, 232–236, https://doi.org/10.1002/pat.1524
47. Ashraf, M.A., Peng, W., Zare, Y. et al. Effects of Size and Aggregation/Agglomeration of Nanoparticles on the Interfacial/Interphase Properties and Tensile Strength of Polymer Nanocomposites. Nanoscale Research Letters, 2018, 13, 214 https://doi.org/10.1186/s11671-018-2624-0
48. Long H., Li M., Han X., Yang X., Fabrication of monodisperse Ag nanoparticles on silica nanospheres and their antibacterial activity, RSC Advances, 2014, 4, 47525–47532. https://doi.org/10.1039/c4ra08418g
49. Milczarek, G., Motylenko, M., Modrzejewska-Sikorska, A., Klapiszewski, Ł., Wysokowski, M., Bazhenov, V.V., Piasecki, A., Konował, E., Ehrlich, H., Jesionowski, T. Deposition of silver nanoparticles on organically-modified silica in the presence of lignosulfonate, RCS Advances, 2014, 94. https://doi.org/10.1039/c4ra08418g